

PREPARATION OF COLOR-CHANGING PACKAGING MATERIAL FOR MONITORING THE FRESHNESS OF CARICA PAPAYA IN REAL-TIME

Tanaya S. Mondal*, Savanta V. Raut and Madhavi U. Bhise

Department of Microbiology, Bhavans College, Andheri West, Mumbai-400 058.

Article Received on
13 November 2024,

Revised on 03 Dec. 2024,
Accepted on 23 Dec. 2024

DOI: 10.20959/wjpr202401-35118



*Corresponding Author

Tanaya S. Mondal

Department of
Microbiology, Bhavans
College, Andheri West,
Mumbai-400 058.

ABSTRACT

Anthocyanin, a natural pigment found in red cabbage, can act as a pH sensitive indicator. A novel intelligent packaging material in the form of thin film was prepared by casting and drying a mixed solution of gelatin, carboxymethyl cellulose (CMC) and xanthan gum, to which anthocyanin was incorporated as the pH indicator. This film can indicate the freshness of fruit through color changes due to the gaseous microbial by-product formed in response to the fruit spoilage. Variations in the three film components were investigated using Fourier transform infrared spectroscopy. Furthermore, the film morphology and structure were evaluated using scanning electron microscopy. Xanthan gum enhanced the water resistance of the gelatin-CMC film and also improved the physical properties like light barrier. The improved activity is due to the enhanced immobilization of anthocyanin dye. The gelatin CMC-xanthan gum-anthocyanin (GCX)

film showed different color changes in response to different pH buffers. It was also found to be sensitive towards gaseous metabolites. When the film was stored with Papaya at room temperature (RT) and 4°C, it showed a color change from green to pink as the fruit started losing its freshness. Hence, this film can be used in monitoring the freshness of fruits in real time.

KEYWORDS: Intelligent Packaging, Anthocyanin, Xanthan gum, Papaya.

1. INTRODUCTION

Food is a fundamental human necessity, and access to healthy, quality food is a basic right. However, food spoilage remains a persistent challenge, leading to significant economic losses

and potential health risks. Spoilage occurs due to inadequate storage conditions, microbial contamination, prolonged shelf life, and environmental factors such as temperature fluctuations, humidity, and exposure to light. Improper handling during transportation and storage further accelerates spoilage, particularly in fruits and vegetables. These perishable items, which continue respiratory activity even after harvest, are especially prone to microbial contamination during transport and storage due to insufficient quality monitoring and faulty packaging techniques (Mohebi *et al.*, 2015; Slavin *et al.*, 2012). Fruits are an essential component of the human diet, providing vitamins, minerals, antioxidants, fiber, and other nutrients. Their quality and safety are critical for consumer health, emphasizing the need for effective spoilage mitigation strategies, such as real-time monitoring systems incorporated into packaging.

Smart or intelligent packaging has emerged as a promising solution to these challenges. Intelligent packaging integrates active materials with intelligent components, allowing the detection and monitoring of food quality changes. Freshness indicators are a key feature of intelligent packaging, providing visual cues about food freshness based on environmental changes, such as pH fluctuations or gas composition. These indicators typically function by detecting metabolites produced during spoilage and reacting with a visible color change (Koshy *et al.*, 2021; Kuswandi *et al.*, 2018). For instance, thin-film intelligent packaging has been developed to monitor the freshness of fruits like *Carica papaya* by detecting pH changes caused by microbial activity (Kaur *et al.*, 2019).

Gaseous metabolites, such as carbon dioxide, ethylene, aldehydes, sulfur-containing volatiles, volatile organic acids, ethanol, and chlorophyll, are among the primary indicators of fruit quality. These compounds accumulate during storage due to microbial spoilage, physiological decay, and mechanical damage, leading to significant changes in fruit freshness, ripeness, and safety. Their increasing concentrations are closely linked to quality deterioration and can be effectively detected using intelligent packaging systems. A notable characteristic of these metabolites is their tendency to decrease the pH of fruits, making pH-sensitive indicators an ideal tool for monitoring spoilage (Shao *et al.*, 2021; Sohail *et al.*, 2018; Ghaani *et al.*, 2016). For example, pH-sensitive indicators embedded in packaging materials or labels provide a simple and cost-effective way to monitor quality, offering real-time feedback to consumers (Warsiki *et al.*, 2018).

Among natural indicators, anthocyanins have proven to be highly effective as pH-sensitive colorimetric sensors. These water-soluble flavonoid pigments exhibit remarkable antioxidant, antimicrobial, and anti-inflammatory properties, along with a halochromic capacity that allows them to change color in response to pH variations. Anthocyanins transition from red to pink, purple/blue, and yellow as pH levels increase, making them suitable for real-time freshness monitoring (*Rotariu et al., 2016; Tavassoli et al., 2021; Hu et al., 2020*). They are derived from natural sources, such as fruits and vegetables, and are considered eco-friendly, non-toxic, and renewable alternatives to synthetic dyes. Their use aligns with consumer preferences for safer, natural food products and satisfies sustainability requirements in the food packaging industry (*Sani et al., 2021; Delgado-Vargas & Paredes-Lopez, 2002; Realini et al., 2014*). Additionally, anthocyanins have been incorporated into biodegradable intelligent packaging systems to enhance the eco-friendliness and functionality of these materials.

Biodegradable packaging matrices, such as gelatin, carboxymethyl cellulose (CMC), and xanthan gum, offer sustainable alternatives to petroleum-based plastics, which contribute to environmental pollution and often contain harmful chemicals like Bisphenol A (BPA) and phthalates (*Rhim et al., 2013; Khazaei et al., 2021*). Gelatin films, known for their transparency and flexibility, can be improved through blending with CMC and xanthan gum to enhance their mechanical and thermal properties. CMC provides a hydrophobic backbone and hydrophilic carboxyl groups that improve the matrix's stability and elasticity, while xanthan gum contributes to flexibility, UV resistance, and water vapor barrier properties (*Boanini et al., 2010; Guo et al., 2014; Ghanbarzadeh & Almasi, 2011*). These materials are readily dispersed in aqueous environments, offering versatility and performance in food packaging applications.

The integration of intelligent packaging systems equipped with natural indicators and biodegradable materials presents a transformative solution to food spoilage challenges. By monitoring the freshness of fruits and vegetables in real time, these systems address consumer demands for safe, high-quality, and eco-friendly food packaging. Intelligent packaging ensures food safety through direct visualization of freshness, enabling informed decision-making and reducing food waste. This innovation has significant implications for the food industry, particularly in enhancing the shelf life and quality of perishable goods (*Kuswandi et al., 2020; Alamdari et al., 2021*).

The development of intelligent packaging systems continues to grow, driven by the need for better quality monitoring and management. By combining natural colorants like anthocyanins with biodegradable matrices, this approach aligns with global sustainability goals while ensuring the safety and satisfaction of consumers. Future research and technological advancements in this field will likely further improve the effectiveness and accessibility of intelligent packaging solutions, supporting the broader aim of reducing food spoilage and its associated economic and environmental impacts (*Sani et al., 2021; Kuswandi et al., 2018*).

This work explores the preparation, characterization, and application of anthocyanin-based intelligent packaging films. The films' functionality is tested on *Carica papaya* under various storage conditions to evaluate their effectiveness as real-time freshness indicators. The findings are expected to provide valuable insights into the integration of natural pigments into intelligent packaging systems and their broader applicability in the food industry.

2. MATERIALS AND METHODS

2.1 Materials

Red cabbage was used for the extraction of anthocyanin pigment and was obtained from the local market of Bhayander East, Thane- 401105. The film composition includes Gelatin, Carboxymethyl cellulose (CMC) and Xanthan gum powder. Other reagents that were utilized includes ethanol, potassium chloride, hydrochloric acid, sodium chloride, sodium hydroxide, sodium acetate, acetic acid, glycerol, boric acid, sodium borate (borax), potassium dihydrogen phosphate, dipotassium hydrogen phosphate, tris base, anhydrous silica gel in desiccator, distilled water, etc. All the reagents were obtained from Loba Chemie Pvt Ltd. All the media like Plate Count agar and Sabouraud Dextrose agar were obtained from HiMedia Pvt. Ltd. The silicone molding tray was bought from Home & Beauty via Amazon.

2.2. Extraction of anthocyanin from red cabbage

The extraction of anthocyanin from red cabbage was carried out using the method previously described by *Chandrasekhar et al., 2012* and *Musso et al., 2018*; with some modifications. The outer layer of the red cabbage was discarded. The rest of the red cabbage was chopped into fine pieces of roughly 1 cm² area. The core of the red cabbage was discarded. The finely chopped red cabbage was then weighed 50g using digital weighing balance. The extraction was carried out by grinding the extract with an appropriate solvent on mortar and pestle. 90% Ethanol was used as the solvent for extraction. The red cabbage and the solvent were used in the ratio of 1:2. After grinding, the extract was filtered through muslin cloth and then with

Whatman filter paper 1. This filtrate was used as red cabbage extract (RCE) for the preparation of the film. This ethanolic extract was stored in the refrigerator for further use [Chandrasekhar *et al.*, 2012; Musso *et al.*, 2018].

2.3. Characterization of the red cabbage extract

2.3.1. Total anthocyanin concentration

The concentration of anthocyanin in the ethanolic RCE was determined using the pH difference method performed as per the method described by Musso *et al.*, 2018. RCE of 0.2 mL volume was mixed with 7 ml of buffer at pH 1.0 and another with 7 ml of a buffer at pH 4.5. The buffer with pH 1.0 was prepared using 0.025 M potassium chloride adjusted with hydrochloric acid. The buffer of pH 4.5 was prepared with 0.4 M sodium acetate adjusted with acetic acid. The absorbance difference at 530 nm (maximum absorption wavelength) of both buffers was measured on a colorimeter (Elico V199) using distilled water as blank. Corrections due to the presence of degraded compounds or interfering substances were done measuring the absorbance at 700 nm. Taking into account that anthocyanins of red cabbage are derived from cyanidin-3-glucoside, concentrations were calculated by using the formula:

Total Anthocyanin Concentration (mg/L) =

$$\frac{\Delta A \times \text{Molecular weight of cyanidin-3-glucoside} \times \text{dilution factor} \times 1000}{\epsilon \times L}$$

Here, ΔA is the difference among absorbance changes at 530 and 700 nm in buffers at pH 1 and pH 4.5. It can be calculated by using the following formula:

$$\Delta A = (A_{530} - A_{700})_{\text{pH } 1.0} - (A_{530} - A_{700})_{\text{pH } 4.5}$$

Molecular weight of cyanidin-3-glucoside is 449.2 g/mol; ϵ is the molar extinction coefficient for cyanidin-3-glucoside ($26900 \text{ cm}^{-1}\text{M}^{-1}$); L is the optical path length (1 cm); 1000 is the conversion factor of grams to milligrams [Musso *et al.*, 2018].

2.3.2. UV-Visible absorption spectra

The RCE was 1:2 diluted with the same solvent that was used for the preparation, i.e., 90% ethanol. The UV-Vis absorption spectra were recorded from 200 to 700 nm [Musso *et al.*, 2018].

2.3.3. Response of the extract to pH changes

0.1 mL of RCE was added to 5 mL of pH buffer of different pH (ranging from pH 2.0 to 11.0). The pH buffers used were acetate buffer to cover the acidic pH (2.0-5.0), phosphate buffer to cover the neutral pH (6.0-8.0) and Borate buffer to cover the alkaline pH (9.0 to 11.0). A spectrum of the extracts exposed to different pH was determined in the range of 410 nm to 670 nm [Chen *et al.*, 2020].

2.3.4 Liquid Chromatography Mass Spectrometry (LCMS) analysis of the extract

LCMS analysis was performed on a HRLCMS-QTOF (High Resolution Liquid Chromatography Mass Spectrometry-Quadrupole Time of Flight) system (Agilent Technologies, USA), consisting of a HiP sampler, a binary pump, a column compartment (Hypersil GOLD C18 100 x 2.1mm³ MICRON), a diode array detector (DAD) and Q-TOF. The mass spectrometer has a dual electrospray ionization source, with positive and negative ionization detection mode. Mobile phase A was consisted of 0.1% formic acid in water in Milli-Q water and the mobile phase B consisted of Acetonitrile. The operating parameters were as followed: flow rate 0.3 mL.min⁻¹; injection volume 3 µL; column temperature 40 °C. The MS analysis was carried out in both positive and negative ionization mode with spectra acquired over a mass range of m/z 120 to 1200. The operating parameters were: nozzle voltage 1.0 kV; drying gas temperature 250 °C; drying gas flow rate 13.0 L.min⁻¹; nebulizing gas pressure 35 psig; The MS data was processed by Agilent Mass Hunter Qualitative Analysis B.06.

2.4. Preparation of the pH sensitive films

Gelatin-CMC-Xanthan-RCE (GCX) films were prepared according to the method of *Hazirah et al.*, 2016 and *Musso et al.*, 2016 with some modifications. Briefly, gelatin (4% w/v), CMC (2% w/v) and Xanthan gum (0.4% w/v) were thermally dissolved, in 50 mL of distilled water, at 80°C in water bath (Equitron, Medica Instrument Mfg. Co.) along with 1.2 mL of glycerol, under stirring condition. The heating was carried out for 30 minutes. After heating, the solution was brought to room temperature. 50 mL of the RCE was then added to the mixture and blended thoroughly. The pH of the solution was adjusted to slightly alkaline with the help of 2 M NaOH and blended properly. This solution was then casted on a silicone molding tray and was dried at room temperature for 2 to 3 days.

Similarly, two other films were made for comparison of the properties. One containing only gelatin and RCE and another containing gelatin, CMC and RCE. Gelatin-RCE (G) film was

prepared by dissolving 4% w/v gelatin and 1.2 mL of glycerol in 50 mL distilled water. The solution was heated at 80°C for 30 mins with continuous stirring. 50 mL of the RCE was added and blended properly. The pH was adjusted to slightly alkaline with the help of 2 M NaOH. This solution was casted on moulding tray and dried at room temperature for 2-3 days.

Gelatin-CMC-RCE (GC) film was prepared by dissolving 4% w/v gelatin, 2% w/v CMC and 1.2 mL of glycerol in 50 mL distilled water. The solution was heated at 80°C for 30 mins with continuous stirring. 50 mL of the RCE was added and blended properly. The pH was adjusted to slightly alkaline with the help of 2 M NaOH. This solution was casted on a molding tray and dried at room temperature for 2-3 days [Musso *et al.* 2016; Hazirah *et al.*, 2016].

2.5 Characterization of G, GC and GCX films

2.5.1 Thickness

Film thickness was measured using a digital gauge (Aerospace digital vernier caliper 150mm). Measurements were done at five random points and an average was taken [Chen *et al.*, 2020].

2.5.2 Moisture content

Moisture content was determined as per the method described by [Chen *et al.*, 2020]. The films were cut in 2 cm x 2 cm dimensions and kept in the hot air oven at 105 °C for 24 h. The samples were weighed before and after drying. The moisture content (MC) was calculated using the following formula:

$$\text{Moisture content (\%)} = 100 \times (\text{Initial weight} - \text{Final weight}) / \text{Initial weight}$$

2.5.3 Solubility test

The solubility of the pH-sensitive films was determined according to the method described by [Prietto *et al.*, 2017]. Briefly, the films were cut in 2 cm x 2 cm dimensions and kept in an oven at 105°C for 24 h. The samples were then immersed in 50 mL of distilled water for a period of 24 h, under shaker and static conditions. The films were then dried at 105 °C until constant weight. Weight of the films were taken before immersing in distilled water and after drying. Water solubility (WS) was calculated using the formula:

$$\text{Water Solubility (\%)} = 100 \times (\text{Initial weight} - \text{Final weight}) / \text{Initial weight}$$

2.5.4 Water vapour permeability

The test was performed as per the protocol described by [Chen *et al.*, 2020]. Briefly, a beaker containing 20 mL distilled water was covered with the film. The beaker was placed in a desiccator containing anhydrous silica gel and the beakers were weighed after every 2 h for 5 times at room temperature. Water Vapour Permeability (WVP) was calculated by using the following formula:

$$\text{Water Vapour Permeability (g/m.s.Pa)} = (\Delta m \times X) / (S \times \Delta P \times t)$$

Here, Δm is the weight difference of film over time (g); X is the film thickness (m); S is the film area (m²); ΔP is the vapor pressure difference of the film (3179 Pa at 22°C); t is time (s).

2.5.5. Elongation at break

Elongation at break (EAB) was calculated by hanging the films of 8 cm x 1 cm dimension from one side and stretching the films from the other side by adding weights. The length of the film was measured after elongation and EAB was calculated using the following formula:

$$\text{Elongation at break (\%)} = \frac{\text{Initial length (cm)} - \text{Final length (cm)}}{\text{Initial length (cm)}} \times 100$$

2.5.6 Morphology

Morphology of the films was determined by scanning electron microscopy (SEM) analysis. The cross-section of the films was observed using FEI Quanta 200 under an accelerating voltage of 10 kV at 500x magnification [Zam *et al.*, 2022].

2.5.7. Fourier Transform infrared spectroscopy (FTIR) analysis of the film

FTIR spectra of films were obtained using a FTIR spectrometer (3000 Hyperion Microscope with Vertex 80 FTIR System, Bruker, Germany) in the range of 4000–400 cm⁻¹ [Chen *et al.*, 2020].

2.5.8. Light transmission and Transparency of the film

UV barrier properties of the films were determined by measuring Transmittance (%) using UV-Vis spectrophotometer (Carry 100 UV-Vis, Agilent Technologies) at a wavelength range of 200 nm to 800 nm [Zam *et al.*, 2022].

Transparency of the film was measured as per the protocol mentioned by Zam *et al.*, 2022. Absorbance of the film were taken at 600 nm and the transparency was determined using the following formula:

Transparency = $-\log T_{600} / X$

Here, T_{600} = absorbance at 600 nm; X = average thickness of the film [Zam *et al.*, 2022].

2.5.9. Response of the films towards various pH

The films were cut into small pieces of 1cm x 1cm dimensions and were exposed to different buffers with pH ranging from 2.0 to 11.0 for 30 secs. The pH buffers used were acetate buffer to cover the acidic pH (2.0-5.0), phosphate buffer to cover the neutral pH (6.0-8.0) and Borate buffer to cover the alkaline pH (9.0 to 11.0).

The total color variance (ΔE) was calculated using the following equation:

$$\Delta E = \sqrt{[(L^* - L)^2 + (a^* - a)^2 + (b^* - b)^2]} \dots \dots \dots (1)$$

where, L , a and b are the values of the film (test), and L^* , a^* , and b^* are the color values of standard white plate (control). Here, ' L ' represents Lightness, ' a ' represents redness/greenness and ' b ' represents blueness/yellowness. The color difference was measured by determining the L , a , b values using photoshop software [Musso *et al.*, 2018; Gao *et al.*, 2022].

2.5.10 Stability test

The films exposed to different pH buffers were stored at room temperature for 28 days. Images were taken on day 0 and day 28 [Prietto *et al.*, 2017].

2.5.11 Durability test

Durability of the films was determined by storing the films at RT for 45 days and then exposing them to various pH buffers.

2.5.12 Response of the films towards gases

The test was performed as per mentioned by Musso *et al.*, 2016. Briefly, each film was faced with gaseous media of acidic pH. This was done by exposing the films to the gaseous atmospheres generated by acetic acid glacial ($C_2H_4O_2$, $pK_a \sim 4.8$). Photographs of films before and after 30 mins of contact were taken [Musso *et al.*, 2018].

2.5.13. Response of the film towards microbial reaction

To determine whether the films are sensitive towards microbial reactions, a test was performed where all the films were cut in rectangular pieces and placed inside a petri dish under sterile conditions. Sterile Nutrient agar and Sabouraud agar blocks were placed on the film such that each film contains a total 4 blocks (one Sabouraud agar block and three Nutrient agar blocks). One nutrient agar block was used as control. The remaining nutrient

agar blocks were inoculated with *Escherichia coli* and *Staphylococcus aureus*. The Sabouraud agar block was inoculated with *Aspergillus niger*. The plates were incubated at room temperature for 24-48 hrs.

2.6 Application of the films for spoilage detection of Carica papaya

2.6.1. Preliminary testing of the film on Papaya

Briefly, the films were cut into rectangular pieces and were placed on a petri dish under aseptic conditions. Fresh Papaya pieces of roughly 2g weight were placed on top of the film. The papaya was then spiked with *Aspergillus niger* spores and the plates were incubated at room temperature for 48 h.

2.6.2. Application of the films on fresh-cut papaya stored at RT

Briefly, a blemish-free papaya was washed and its inedible parts were removed. The cut pieces were placed on clean containers with a lid. The containers had approximately 200 g fresh-cut papaya each. The cut colorimetric films were attached on the inner side of the lid. The containers were then stored at room temperature and at every 0h, 2h, 4h, 6h, 8h, 24h and 48h, color, texture, odor, pH, acidity, microbial load of the papaya was noted and the color change of the film was observed.

The pH was determined by making a slurry of 10 g papaya with mortar and pestle. The pH meter (Universal Enterprises UD-95) probe was then dipped into it and the readings were noted.

Acidity was determined by homogenizing 1g of the sample and 10 mL distilled water on mortar and pestle. The homogenate was filtered using Whatman filter 1. The filtrate was titrated with 0.1N NaOH with 0.1% phenolphthalein indicator. Endpoint was determined by color change from colorless to pink.

Microbial load was determined by performing Miles and Misra on sterile plate count agar (for bacterial count) and Spread plate method on sterile Sabouraud agar (for fungal load). Briefly, 1 g sample was weighed and inoculated in 10 mL of sterile saline under aseptic condition. The sample was homogenized using vortex and suitably diluted. Viable count of the diluted sample was determined by the above-mentioned techniques [Rong *et al.*, 2023].

2.6.3. Application of the films on fresh-cut papaya stored at 4°C

A blemish-free papaya was washed and its outer layer was removed. The cut pieces were placed on clean containers with a lid. The containers had approximately 200 g fresh-cut papaya each. The cut colorimetric films were attached on the inner side of the lid. The containers were then stored in a refrigerator (4°C) and was monitored daily till a color change in the film was observed. The color, texture, odor, pH, acidity, microbial load of the papaya was noted and the color change of the film was observed. For the test of pH, acidity and microbial load, refer to section 2.6.2 [Rong *et al.*, 2023].

2.6.4 Application of the films on fresh-intact papaya

The surface of the blemish-free, fresh whole papaya was disinfected with alcohol. The surface was then swabbed with the 100 µL of the spore suspension of *Aspergillus niger*. The films were cut into small pieces and were applied on the swabbed region. The spiked papaya was then incubated at RT till the change in color of the films were observed. The load after spoilage was then determined by performing spread plate on sterile Sabouraud agar.

3. RESULT AND DISCUSSION

3.1. Extraction of anthocyanin from red cabbage

Firstly, anthocyanin extraction and yield from red cabbage (*Brassica oleracea*) was investigated. In this work, a simple and cost-effective method was used to extract anthocyanin from red cabbage by ethanol extraction, followed by filtration. This is a version of Solid-Liquid Extraction (SLE), a method commonly used for extraction of anthocyanins from plant matter. The technique separates mixtures of solid compounds based on their solubility in a particular solvent. Anthocyanins are polar compounds making them soluble in polar solvents such as water, ethanol, and methanol. Anthocyanins are known to degrade at high temperature, so processing is preferably conducted at low temperature.



Figure 3.1: Anthocyanin extracted from red cabbage by Solid-liquid extraction process.

3.2. Characterization of the red cabbage extract

3.2.1 Total anthocyanin concentration

Total anthocyanin concentration was calculated as per the method mentioned by Musso *et al.*, 2018. Absorbance of the extract of pH 1.0 and 4.5 were taken at 530 nm and 700 nm. These two wavelengths were selected because 530 nm is the maximum absorption wavelength of cyanidin-3-glucoside, the essential component of anthocyanin pigment, and the corrections due to the presence of degraded compounds or interfering substances were done measuring the absorbance at 700 nm. The total anthocyanin concentration in terms of cyanidin-3-glucoside was calculated using the formula mentioned in 2.3.1. and was found to be 15 mg%. The value was found to be much higher compared to the value obtained by Musso *et al.*, 2018. This is because grinding on mortar and pestle causes lesser heat generation compared to mixer/chopper.

3.2.2. UV-Visible absorption spectra

Spectral characterization of the extract was done by measuring absorbance in the wavelength range of 200 to 700 nm at an interval of 20 nm.

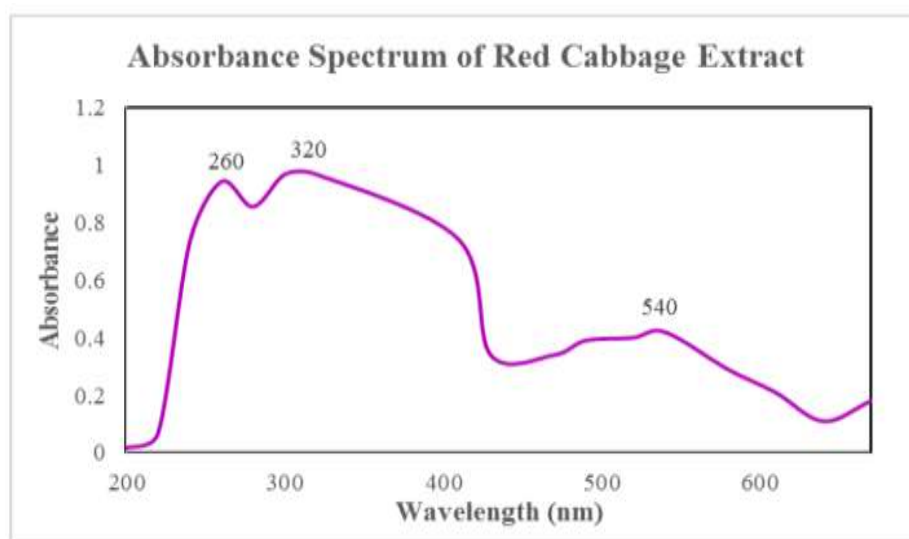


Figure 3.2: Absorbance spectrum of Red Cabbage extract.

Peaks were observed in 260 nm, 320 nm and 540 nm. This confirms the presence of anthocyanin in the extract (Figure 3.2). A typical UV-Vis spectrum of an anthocyanin shows two basic clusters of absorbance, the first one at a wavelength region of 260–280 nm (UV region) and the other one at 490–550 nm (visible region). Apart from them, an additional peak is observed in the wavelength range of 310–340 nm whenever the sugar moiety is

acylated. This indicates that the extract contains acylated form of anthocyanin [Saha *et al.*, 2019].

3.2.3 Response of the extract to pH changes

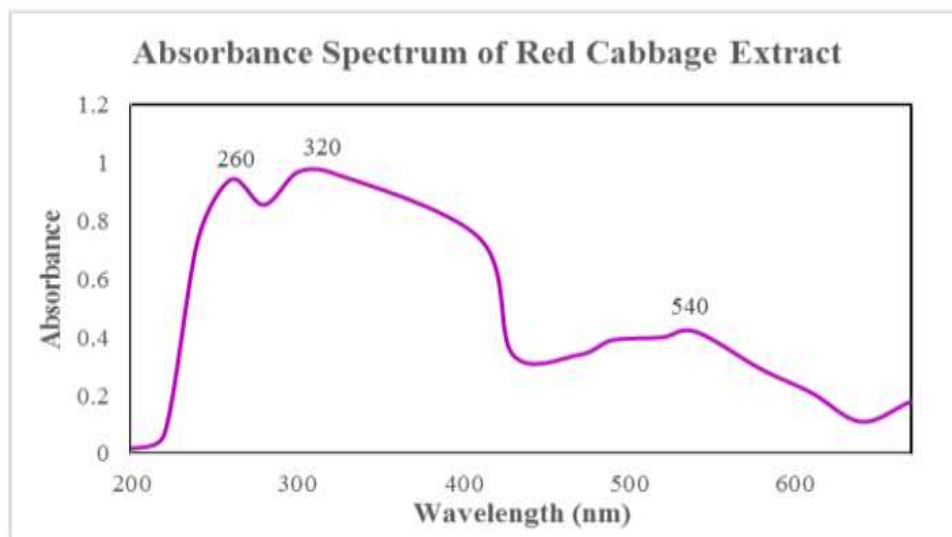


Figure 3.3: Red Cabbage Extract exposed to various pH buffers.

The colour variations of the RCE at different pH was determined to validate its use as pH indicator. In *figure 3.3*, it can be observed that in pH range 1.0 to 4.0, the colour of the anthocyanin is red-pink. This is due to the formation of flavonoid cation. In the pH range of 5.0-9.0, quinoidal base starts to form, whereas in the pH 10.0-11.0, green coloured chalcone was formed. Research has demonstrated that anthocyanins decompose rapidly and that its chemical properties are unstable. The stability of anthocyanins varies with differences in pH, storage temperature, enzymes, and the light, and oxygen conditions of their environment. When the structure and concentration of anthocyanins differed, the differences in stability were found to be enormous. In response to this, researchers [Clifford, 2000] determined that in dilute acid solutions anthocyanins exist in the form of flavonoid cations, and that double bonds are prone to extended conjugation, forming a colourless pseudo alkaline and a balanced reaction of red flavonoid cations. Anthocyanins are more stable in acidic than in alkaline solutions. Under acidic conditions anthocyanins form four substances: colourless chalcones, colourless carbinol pseudo-base, red flavonoid cations, and blue quinoidal alkali. The four substances form a dynamic equilibrium. When the solution's alkalinity increases, the nucleophilic reaction between the red flavonoid cations and water forms colourless carbinol. This is because the total amount and concentration of the red flavonoid cations are reduced and the colour intensity is correspondingly reduced. Consequently, when anthocyanins are in

an acidic medium, the flavylum cations play a major role and the solution appear red. With an increase in pH, the anthocyanins become quinoid alkali caused by a loss of cations from the carbon and oxygen ring, and the solution appears blue or green [Khan *et al.*, 2011]. This reaction was confirmed by measuring the λ_{max} of the extract exposed to different pH buffers. It can be observed that the λ_{max} shifted from 490nm to 600nm, indicating formation of quinoidal base from flavonoid cation.

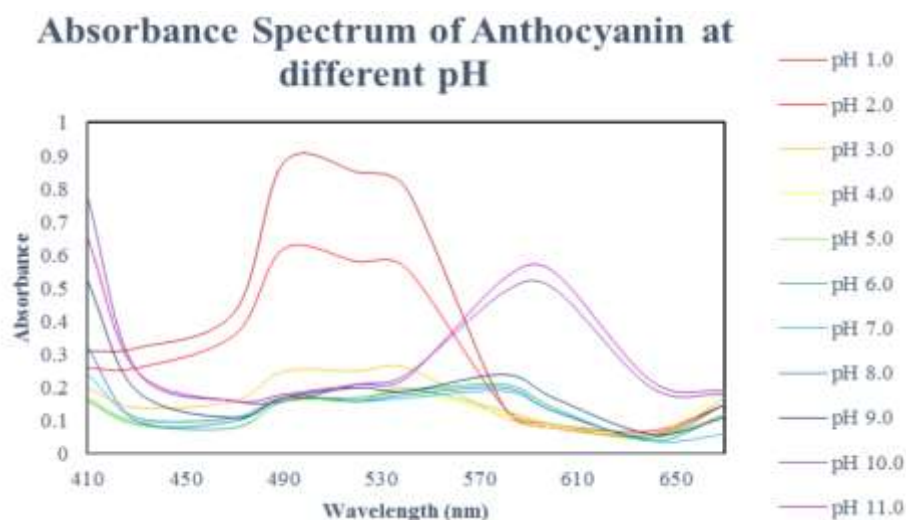


Figure 3.4: Absorbance Spectrum of anthocyanin at different pH.

3.2.4. LCMS analysis of the extract

Further the LCMS analysis showed that the types of anthocyanin present in the extract are: cyanidin-3-glucoside, cyanidin 3-diglucoside-5-glucoside and cyanidin 3-(p-coumaroyl) diglucoside-5-glucoside.

Table 3.1: LCMS results of the extract.

Sr. No.	Name	Formula	Retention time	Score	m/z
1	Cyanidin-3-glucoside	C ₂₁ H ₂₁ O ₁₁	5.401	79.22	494.108
2	Cyanidin 3-diglucoside-5-glucoside	C ₃₃ H ₄₁ O ₂₁	3.549	84.94	772.205
3	Cyanidin 3-(p-coumaroyl) diglucoside-5-glucoside	C ₄₂ H ₄₇ O ₂₃	6.26	81.76	918.2427

3.3 Appearance of the pH sensitive film

The pH sensitive films were then prepared by casting and drying method. Three films were made, the first one (G) containing gelatin and anthocyanin; the second one (GC) containing gelatin, CMC and anthocyanin; and the third one (GCX) containing gelatin, CMC, xanthan

gum and anthocyanin. The appearance of the films is in the *Figure 3.5*. The G film is slight pinkish purple and the GC and GCX films are light green in colour.

Table 3.2: The colour parameters including *L*, *a*, *b* and Colour Variance (ΔE) of the films.

Film	L	a	b	ΔE
G	68.61	1.53	11.93	33.62
GC	63.63	-5.08	27.77	46.04
GCX	67.51	-5.19	26.56	42.28

Here, 'L' represents Lightness, 'a' represents redness/greenness and 'b' represents blueness/yellowness.

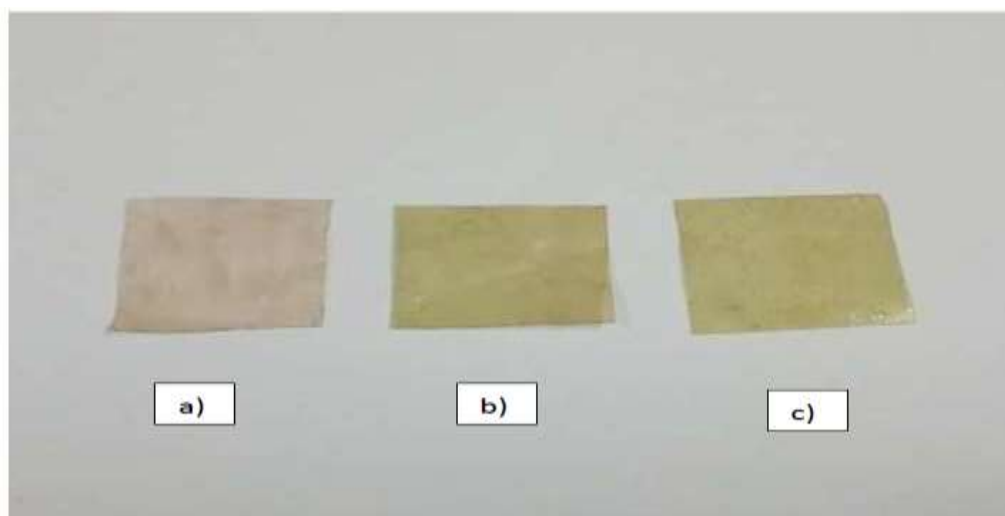


Figure 3.5: Appearance of the film after drying for 48 h. a) G b) GC c) GCX.

3.4 Characterization of the films

3.4.1. Thickness

The thickness of the films was measured using Aerospace 150 mm digital vernier calliper. The thickness was measured at 5 different points. Thickness is an important parameter that is related to the barrier property of the films. GCX film showed the highest thickness of 0.14 mm, whereas G film showed the lowest out of all (Table 3.3). These results suggested that xanthan gum formed a compact film network with gelatin and CMC molecules due to crosslinking within the film matrix, thus, resulting in increased thickness value. Crosslinking aids in immobilization of the anthocyanin pigment, hence GCX film showed better colour out of all (discussed in the later part).

Table 3.3: Thickness, Moisture content (MC), Water solubility (WS) under static and shaker condition, Water vapour permeability (WVP), Elongation at break (EAB) of the films.

Films	Thickness (mm)	MC (%)	WS (%)	WS (%)	WVP (10^{-11} g/msPa)	EAB (%)
G	0.06	21.43 ± 7.15	55 ± 5	66.67	1.16 ± 0.62	37.5
GC	0.12	18.78 ± 6.25	38.09 ± 4.77	42.86	2.49 ± 1.57	25
GCX	0.14	12.5	42.86	42.86	1.78 ± 0.99	11.3

3.4.2 Moisture content (MC)

The moisture content was calculated by measuring the weight of the films before and after drying at 90°C for 24 h. Incorporation of xanthan gum not only increased the thickness, but also enhanced the other physical properties (Table 3.3). Test for moisture content of the films showed that GCX had the least moisture content of 12.5%, followed by GC ($18.78 \pm 6.25\%$) and G ($21.43 \pm 7.15\%$). Xanthan gum might interact with gelatin via hydrogen bonds that block hydroxyl positions capable of associating with water to reduce moisture content in gelatin films. Also, the anthocyanin present can bind to the hydroxyl position thereby inhibiting the binding of water molecules. Similar mechanism was followed by CMC in the GC film.

3.4.3 Water Solubility test (WS)

Bio-based films need to be durable for packaging with minimum solubility. Solubility gives an indication of the film's water affinity. Water solubility was checked under static as well as shaker condition (Table 3.3). Results after 24h showed that the films were more soluble in shaker condition than static. Incorporation of xanthan gum improved the water resistance; and the film containing xanthan gum was found to be equally soluble in static as well as shaker condition with water solubility of 42.86%. The film containing gelatin showed the most solubility under both static as well as shaker conditions.

3.4.4 Water Vapour Permeability Test (WVP)

Water Vapour Permeability is another factor that must be taken into consideration during food packaging. Lesser the value, better the bioplastic. Table 3.3 shows the results of the water vapour permeability test. Gelatin film (G) showed the least water vapour permeability ($1.16 \pm 0.62 \times 10^{-11}$ g/msPa), followed by GCX ($1.78 \pm 0.99 \times 10^{-11}$ g/msPa) and GC ($2.49 \pm 1.57 \times 10^{-11}$ g/msPa). As per the study by *de Carvalho and Grosso (2004)* where crosslinking

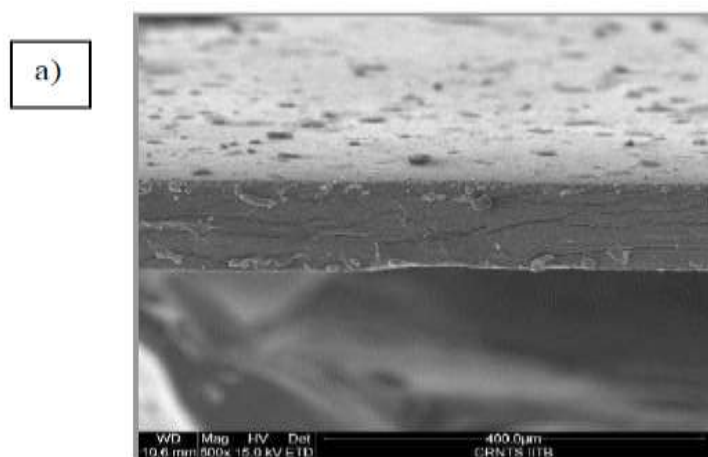
reactions influenced the moisture diffusion coefficient within the gelatin's network, indicating structural changes in the polymeric matrix after crosslinkers were introduced to gelatin films. Thus, in the present study, the addition of xanthan gum to gelatin-CMC film appears to have changed the structure of the polymeric matrix affecting the moisture diffusion coefficient within the gelatin-CMC network as influenced by crosslinking reactions within the composite films. Addition of xanthan gum improved the water vapour barrier property compared to the gelatin-CMC film. This helps in keeping food fresh for longer time.

3.4.5 Elongation at break

Elongation at break was determined manually by adding the weights from one side and was determined by the action of the gravitational force. Incorporation of xanthan gum had significantly decreased the elongation at break compared to the other two films (*Table 3.3*). This result matches the result obtained by *Hazirah et al., 2016*. This might be due to the availability of the free OH group in the film matrix. Lower the elongation at break, better is the mechanical property of the film.

3.4.6 Morphology

The cross-sections of the films were observed in Environment Scanning Electron Microscope (ESEM) under 500x magnification (*Figure 3.6*). The images reveal that the addition of xanthan gum in the film reduced the smoothness.



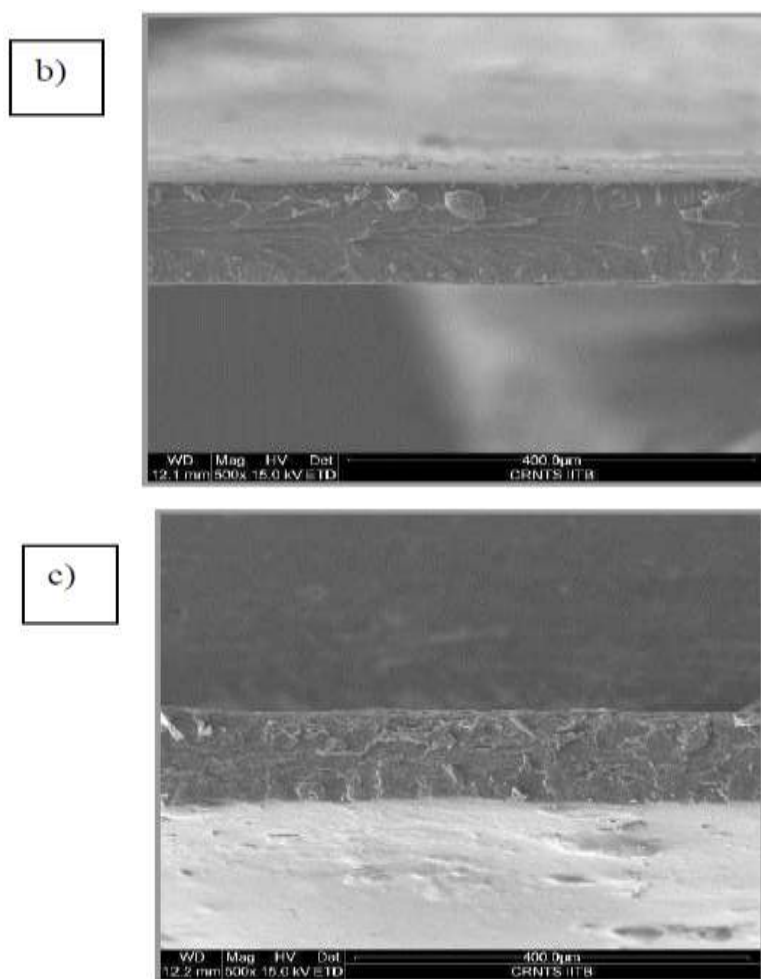


Figure 3.6: Morphology of the films under 500X. a) G, b) GC and c) GCX.

3.4.7 Fourier Transform Infrared (FTIR) analysis of the film

The FTIR spectrum of the three films was determined in the range of 400 to 4000 cm^{-1} (Figure 3.7). FTIR analysis of the film shows the bond formation between the components of the film. In all the three films, free OH stretching was observed, indicating the presence of alcohol group. This was indicated by peaks in the region 3670 cm^{-1} to 3550 cm^{-1} . GCX had the lowest intensity, hence showed the best mechanical properties out of all. Normal polymeric OH stretch was detected in the region of 3400 cm^{-1} to 3200 cm^{-1} . Methoxy, methyl ether stretch was observed in GC film in the range of 2850 cm^{-1} to 2815 cm^{-1} . Secondary amine with N-H bend is present in all the three films, indicating the amino group of gelatin. This was detected in the range of 1650-1550 cm^{-1} . Several peaks in the region of 2000 to 1600 cm^{-1} indicates the compounds are aromatic. Peak in the region of 2500 to 200 cm^{-1} indicates the presence of triple bond. Presence of carbonate ion in GC and GCX was detected in the range of 880-860 cm^{-1} . All these information conclude that all the three films contain aromatic compound with free hydroxy group [Nandiyanto *et al.*, 2019]. Although the hydroxy

groups are present in all the three films, the incorporation of xanthan gum decreased the intensity, thereby making GCX the best film out of all.

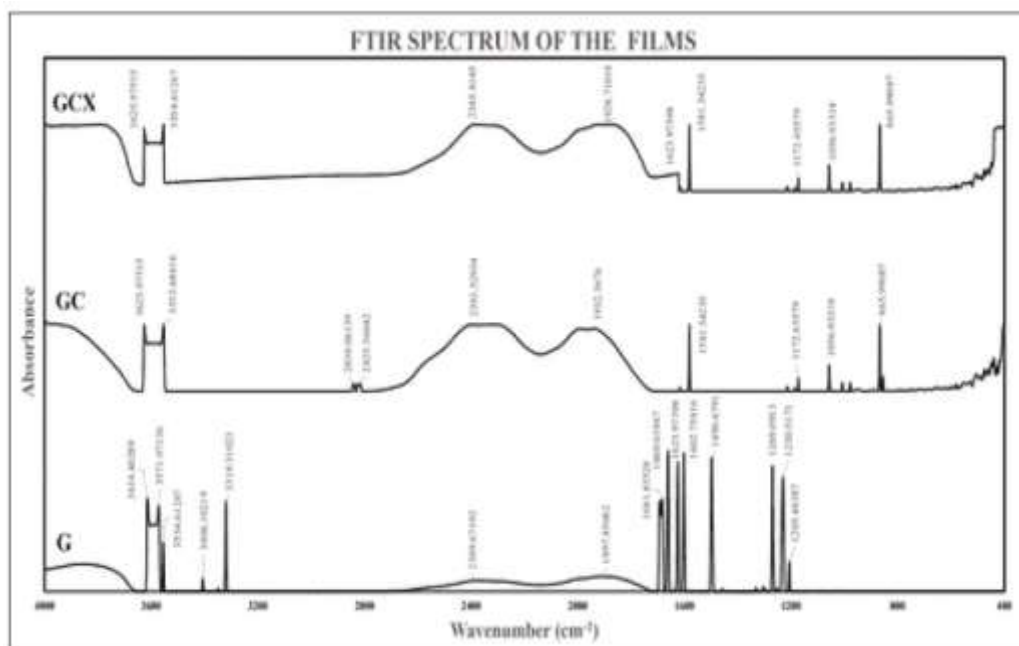


Figure 3.7: FTIR spectrum of the films: G, GC and GCX.

3.4.8 Light Transmission and Transparency test

Light Transmission of all the three films was determined by measuring the Transmittance at various wavelength (Figure 3.8). G film showed the maximum mean transmittance i.e., 13.712 % in the UV range (200 to 400 nm) and GCX film showed the least value of 4.873 %. Low UV transmittance is a key factor in food packaging as UV light could be detrimental for food storage. Thus, it indicates a good UV barrier property. However, from the orange region (> 630 nm), a contrast in the results was observed. GCX showed the maximum mean transmission (80.241 %) and G showed the least value (76.660 %). But the longer wavelengths don't have much effect on food. Only the UV and short wavelength visible light transmission deteriorates the quality of food by causing the oxidation of lipids. Also, the improved cross-linking due to the presence of xanthan gum has decreased the transparency of the film to 5.854%. Therefore, it showed better light barrier property (Table 3.4).

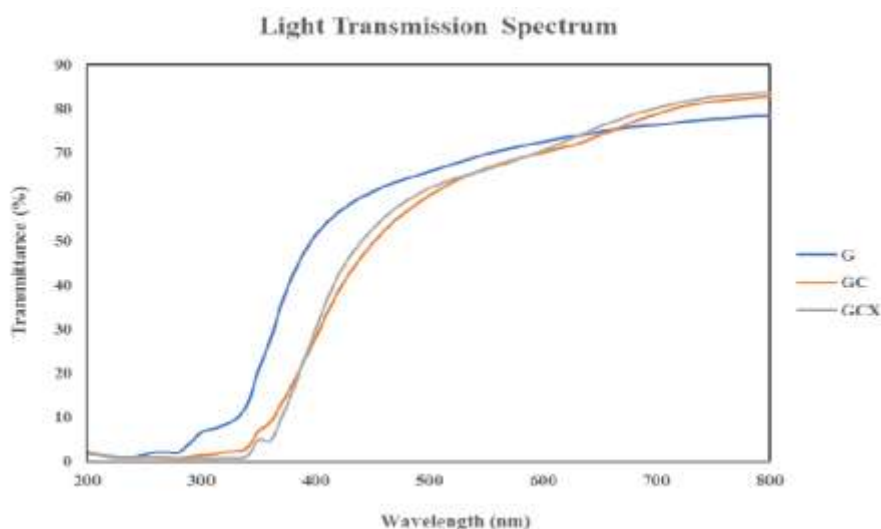


Figure 3.8: Transparency of the films: G, GC and GCX.

Table 3.4: Transparency of the films.

	G	GC	GCX
Transparency (%)	14.262	6.768	5.854

3.4.9 Response of the films towards various pH

Response of the film towards various pH was determined by dipping the films in different pH buffers (Table 3.5). Observations were made after 15 mins and the colour variance (ΔE) was determined. It can be observed that xanthan gum addition improved the colour formation. This is due to the immobilization of more amount of anthocyanin than the rest of the films.

Table 3.5: ΔE of all the films at various pH.

pH	G					GC					GCX				
	Images	L	a	b	ΔE	Images	L	a	b	ΔE	Images	L	a	b	ΔE
1		47	54	3	75.72		74	18	20	37.42		55	52	14	70.18
2		75	15	3	29.31		71	8	24	38.48		63	11	15	41.41
3		77	12	4	26.25		68	4	29	43.37		62	10	13	41.39
4		77	9	3	24.88		69	3	23	38.72		62	5	18	42.34
5		76	7	5	25.50		62	2	28	47.24		57	1	20	47.43
6		76	3	9	25.81		63	-2	27	45.85		63	-3	20	42.17
7		78	4	9	24.10		63	0	25	44.65		59	0	27	49.09
8		80	-2	13	23.94		64	-3	29	46.32		58	-5	33	53.65
9		79	-9	14	26.80		57	-8	36	56.65		58	-15	37	57.95
10		77	-14	12	29.49		62	-9	33	51.13		40	-16	41	63.66
11		56	-37	15	59.41		61	-10	29	49.62		45	-27	39	72.63

Here, 'L' represents Lightness, 'a' represents redness/greenness and 'b' represents blueness/yellowness.

3.4.10 Stability test

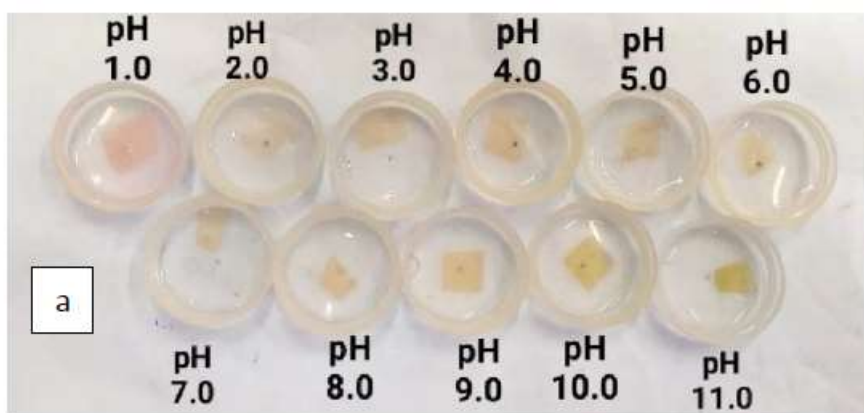
Stability of the film was measured by storing the above-mentioned exposed films at RT for 28 days (Table 3.6). It can be observed that the chalcone formation eventually turned the pigment from green to yellow. But out of the three GCX film is the most stable.

Table 3.6: Stability test of the films.

		pH 1	pH 2	pH 3	pH 4	pH 5	pH 6	pH 7	pH 8	pH 9	pH 10	pH 11
G	0 th day											
	28 th day											
GC	0 th day											
	28 th day											
GCX	0 th day											
	28 th day											

3.4.11 Durability of the films

Durability of the films were tested after exposing the films to different pH buffers on the 45th day after preparation. It can be observed in the figure 3.9 that GCX is the most durable out of all as it showed the colours like a freshly prepared one.



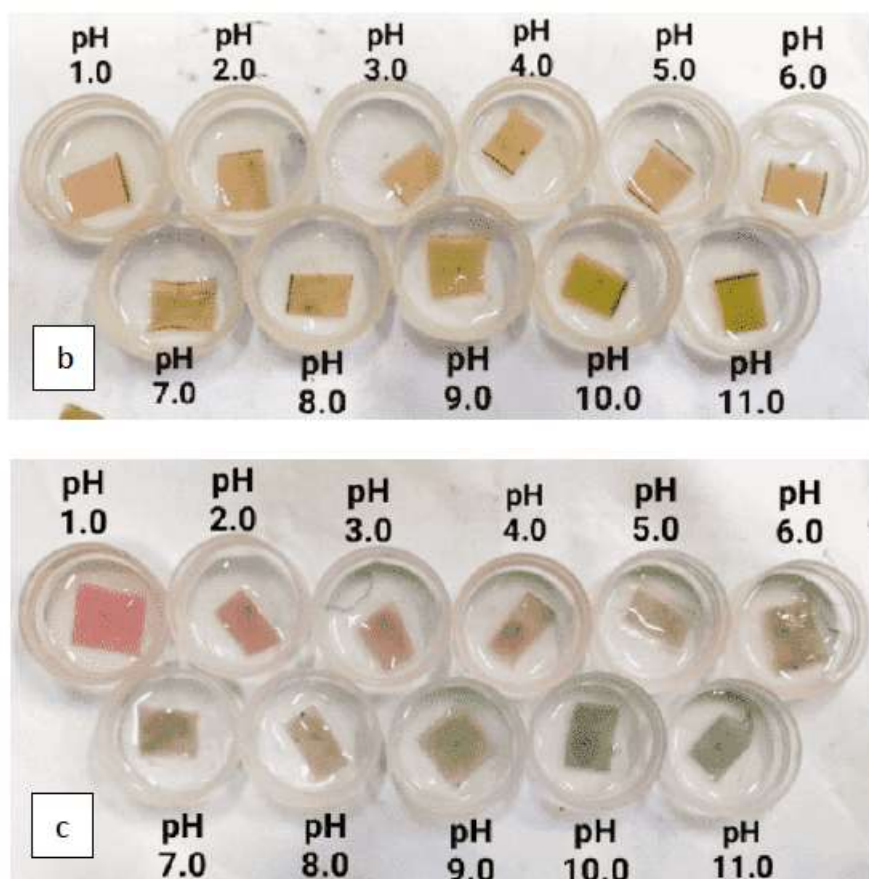


Figure 3.9: Response of the films to the pH buffers after 45 days. a) G, b) GC, and c) GCX.

3.4.12 Response of the films towards gases

For working of the freshness indicator, it must be sensitive to gaseous metabolites. Hence, to check that, the films were exposed to volatile vapours of acetic acid. After 30 mins, GCX showed the darkest colour out of all, indicating its high sensitivity (*Figure 3.10*)

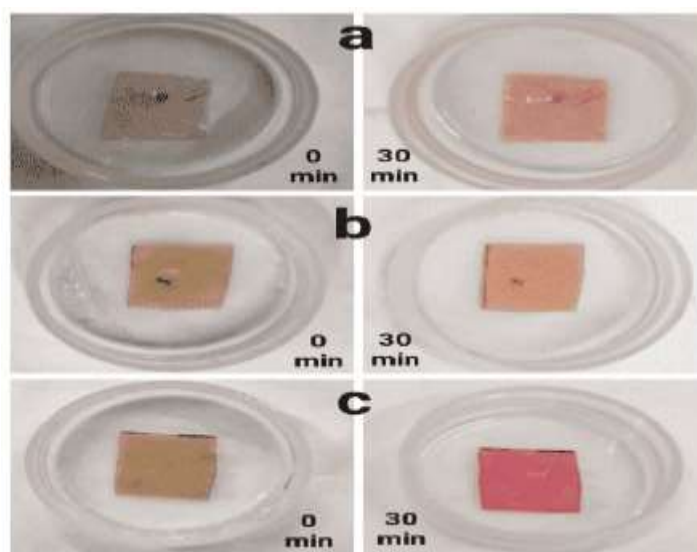


Figure 3.10: Effect of volatile acetic acid on a) G, b) GC and c) GCX.

3.4.13 Response of the films towards microbial reactions

To check whether the films were responsive toward microbial reactions, solid agar medium were placed onto the films and inoculated with different cultures (*Figure 3.11*). The control agar block without any culture showed negative result as there was no change to pink colour. Whereas, the tests or the inoculated ones produced acidic metabolites due to microbial fermentation of sugar in the medium. These metabolites were sensed by the films and the colour tuned to pink near the agar block.

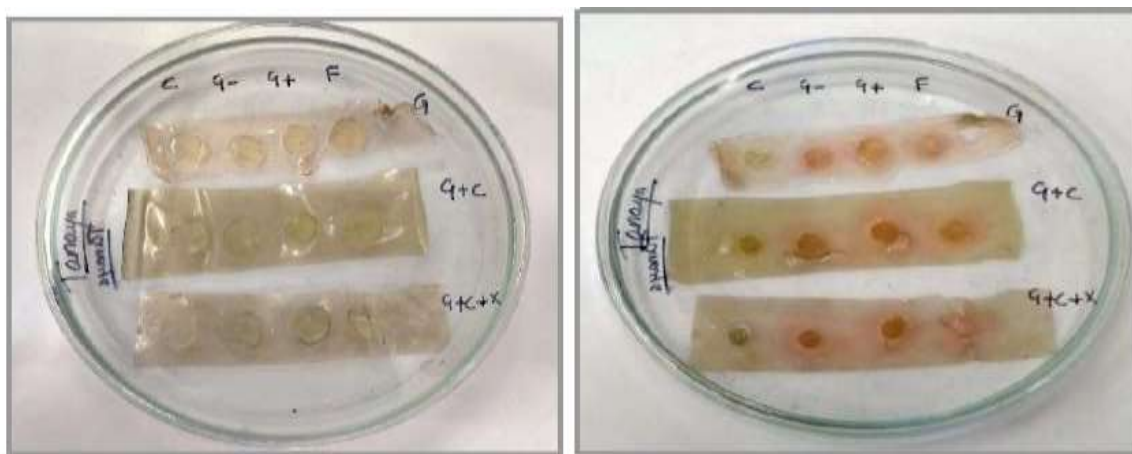


Figure 3.11: Response of the films G, GC and GCX towards the microbial reactions. Here, C= control (uninoculated), G- = *E. coli*, G+ = *S. aureus*, F = *A. niger*. (Left – 0h, Right – 24h).

3.5 Application of the films for monitoring the spoilage of *caraica papaya*

3.5.1 Preliminary testing on papaya

To check the activity on Papaya, a preliminary test was performed. In that test, the papaya pieces were spiked with the spore suspension of *A. niger*. *Figure 3.12* shows that the pH of the papaya did not affect the film, indicating the role of metabolites in the reaction.





Figure 3.12: Spiked papaya at 30min (above) and 24h (below).

3.5.2 Application of the films on fresh-cut papaya stored at RT

Application of the film on Papaya stored at RT showed a colour change within 24 h. This corresponds to a pH change to 3.5 and acidity to 0.161%. The SPC was found to be 5.25×10^7 cfu/g. As per FSSAI, the cut or minimally processed fruits must not contain bacterial load of more than 10^7 /g. Our result corresponds with the standard, indicating a really good sensitivity of the film.

Table 3.7: Sensory evaluation of the fruit stored at RT and colour variance (ΔE) of the films.

Time (h)	Colour	Odour	Texture	G	ΔE	GC	ΔE	G CX	ΔE
0	Orange	Sweet	Hard		15.12		23.89		33.86
2	Orange	Sweet	Hard		20.09		17.17		30.21
4	Orange	Sweet	Hard		24.92		31.48		38.94
6	Orange	Sweet	Hard		18.03		25.71		26.25
8	Reddish orange	Sweet	Hard		18.71		25.06		32.35
24	Orangish red	Slight fermented	Slight soft		16.81		24.88		46.07

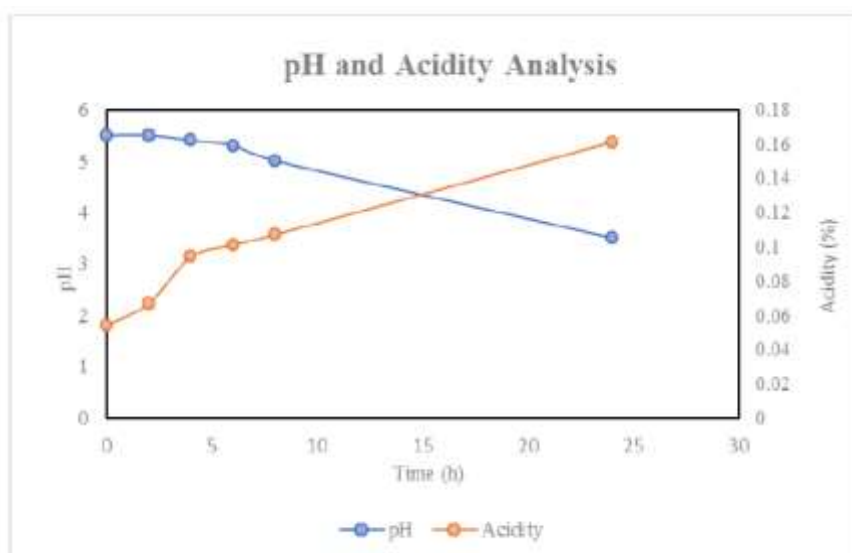


Figure 3.13: pH and Acidity of Papaya stored at RT.

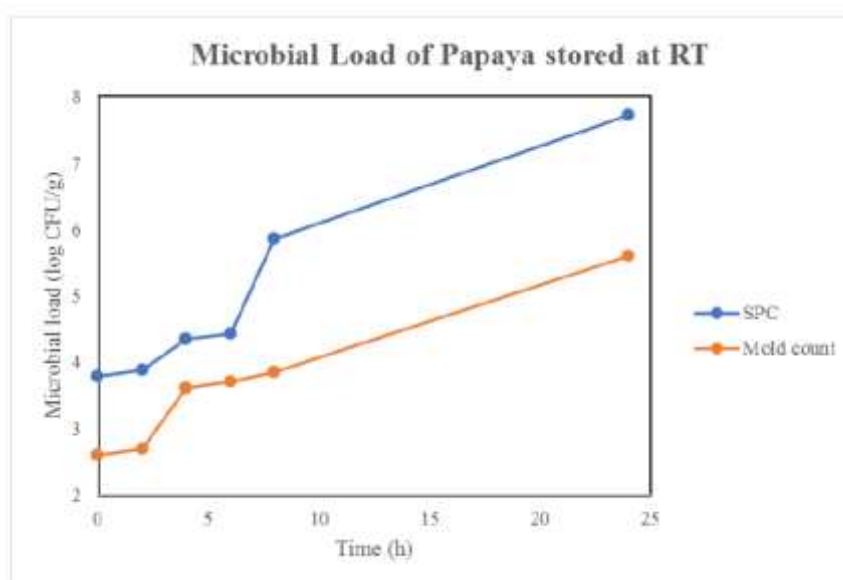











Figure 3.14: Microbial load of Papaya stored at RT.

3.5.3 Application of the films on fresh-cut papaya stored at 4°C

The freshly-cut papaya was stored in the refrigerator and at different intervals the films and the fruit were evaluated.

Table 3.8: Sensory evaluation of papaya stored at 4°C and colour variance (ΔE) of the film.

Day	Colour	Odour	Texture	G	ΔE	GC	ΔE	GCX	ΔE
0	Orange	Sweet	Hard		15.12		31.13		30.82
1	Orange	Sweet	Hard		20.09		27.21		38.74
2	Orange	Sweet	Hard		24.92		30.54		42.22
3	Reddish orange	Sweet	Hard		18.03		29.4		41.69

4	Orangish red	Slight fermented	Slight soft		13.71		18.45		64.46
5	Orangish red	Slight fermented	Soft		18.42		21.37		47.67
7	Orangish red	Fermented	Mushy		16.81		18.70		46.17

Colour change was observed within 7 days. This corresponds to a pH change to 3.5 and acidity to 0.161% (Table 5.18). The SPC was found to be 1.4×10^7 cfu/g (Table 5.19).

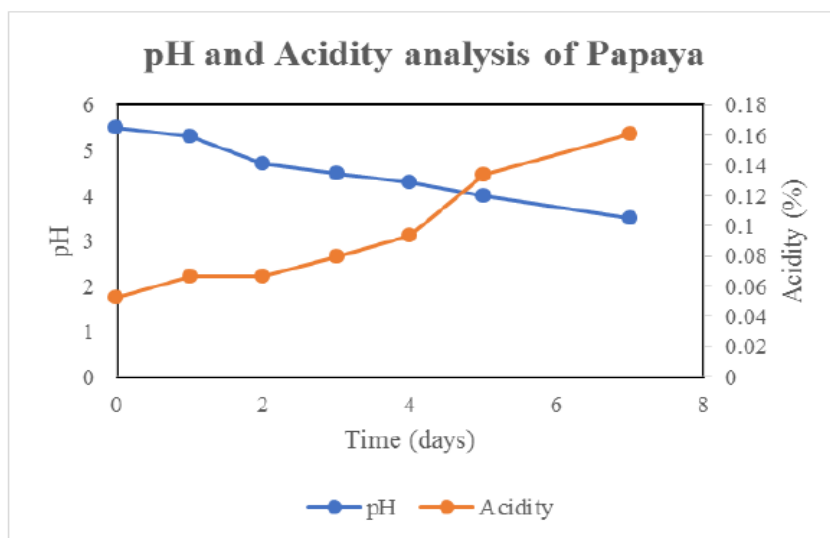


Figure 3.15: pH and Acidity of Papaya stored at 4°C.

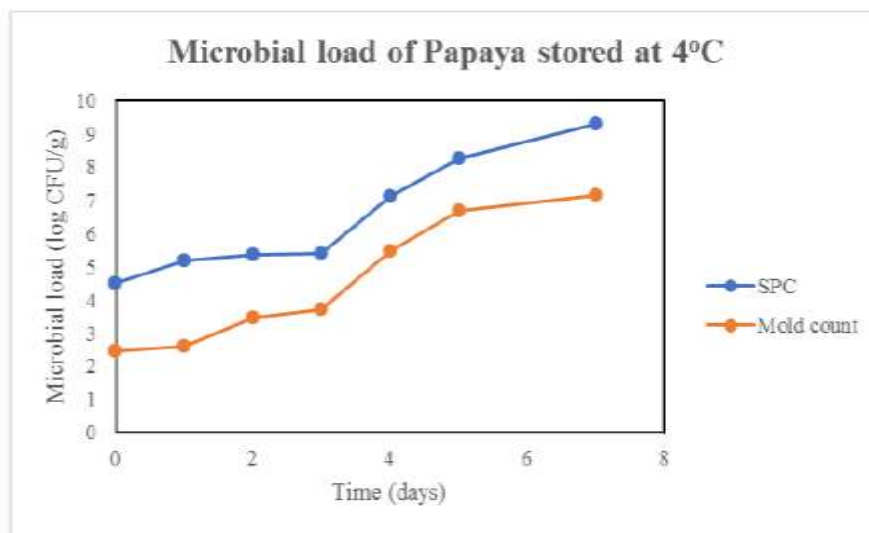


Figure 3.16: Microbial load of Papaya stored at 4°C.

3.5.4 Application of the films on fresh-whole papaya

Application on intact papaya was done by spiking the spore suspension containing 1.65×10^4 CFU/mL. After 24h, the colour of the film changed to pinkish green and on the 48th day, the colour changes completely to pink with the mould count of 1.45×10^5 CFU/mL.

Table 3.9: Microbial load of spiked papaya.

Time	Average CFU/mL
0h	1.65×10^4
48h	1.45×10^5

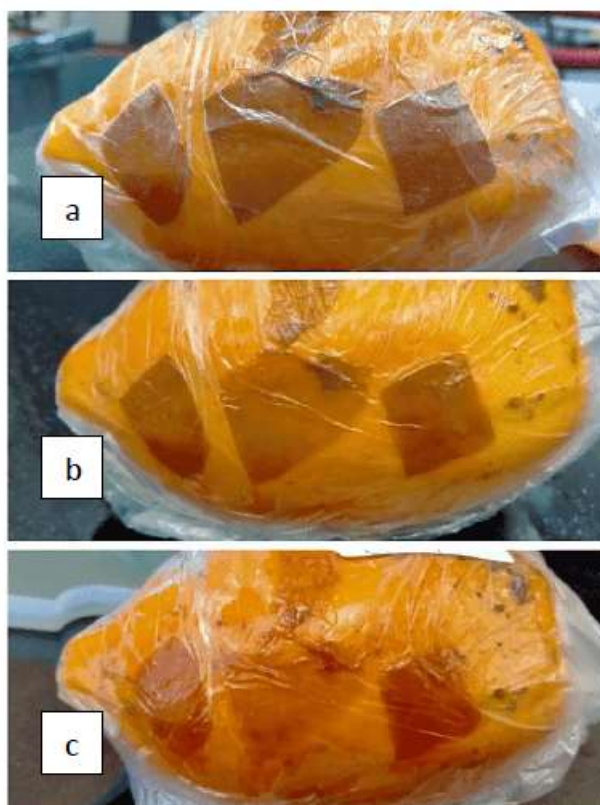


Figure 3.17: Result observed on whole papaya at a) 0h, b) 24h, c) 48h. (Left to right- G, GC, GCX)

4. CONCLUSION

To track the freshness of fruit in real-time during transportation, intelligent packaging materials were prepared based on gelatin, CMC and xanthan gum. Anthocyanin obtained from red cabbage, by solid-liquid extraction process, was used as a natural indicator. The presence of anthocyanin was confirmed by determining of the absorption spectrum using UV-Vis spectrophotometer. The concentration of anthocyanin in terms of cyanidin-3-o-glucoside was found to be 15mg%. The anthocyanin was incorporated into three film blends of gelatin

(G), gelatin-CMC (GC) and gelatin-CMC-xanthan gum (GCX), respectively. These three films were compared for various, physical, mechanical and chemical properties. GCX film showed the highest water barrier property, lowest water solubility and moisture content. This is due to its increase in thickness. Further, microscopic analysis of the cross-section reveals the compatibility of the xanthan gum with gelatin, CMC and anthocyanin. The optical properties like light transmission and transparency of the film indicates that xanthan gum reduced the transparency of the film and thereby increased the UV barrier property of the film. Moreover, addition of xanthan gum improved the sensitivity of the film toward different pH buffers, increased the durability and stability of the film. The application of the film on monitoring the freshness of papaya, stored at room temperature (RT) and 4°C, indicated that the films were able to detect the microbial count of 10^7 cfu/g. The collective data suggests that the gelatin-CMC-xanthan gum-anthocyanin containing film can be used for monitoring the freshness of the food products in real-time, thereby ensuring the safety of the consumers.

5. Future prospects

This project studied the combined effect of gelatin, CMC, xanthan gum and anthocyanin for monitoring freshness of fruit in real time. Analysis such as X-ray diffraction (XRD), thermogravimetric test should be carried out to examine the chemical composition and thermal durability of the films, respectively. Tensile strength can be determined to measure the strength of the film. The CO₂ liberated during microbial metabolism has to be quantitatively estimated in real time to study the sensitivity of the film. Also, the antioxidant activity of the film has to be tested. Antimicrobial testing can be done by comparing the films with traditional packaging materials. This strategy can be applied for the preparation of biosensor that can quantitatively estimate the spoilage level in real-time, thereby ensuring the safety to the consumers.

6. REFERENCES

1. Alamdari, N. E., Aksoy, B., Aksoy, M., Beck, B. H., & Jiang, Z. A novel paper-based and pH-sensitive intelligent detector in meat and seafood packaging. *Talanta*, 2021; 224: 121913.
2. Boanini, E., Rubini, K., Panzavolta, S., & Bigi, A. Chemico-physical characterization of gelatin films modified with oxidized alginate. *Acta Biomaterialia*, 2010; 6: 383–388.

3. Chandrasekhar, J., Madhusudhan, M. C., & Raghavarao, K. S. M. S. Extraction of anthocyanins from red cabbage and purification using adsorption. *Food and bioproducts processing*, 2012; 90(4): 615-623.
4. Chen, H. Z., Zhang, M., Bhandari, B., & Yang, C. H. Novel pH-sensitive films containing curcumin and anthocyanins to monitor fish freshness. *Food Hydrocolloids*, 2020; 100: 105438.
5. Clifford, M. N. Anthocyanins—nature, occurrence and dietary burden. *Journal of the Science of Food and Agriculture*, 2000; 80(7): 1063-1072.
6. de Carvalho, R. A., & Grosso, C. R. F. Characterization of gelatin based films modified with transglutaminase, glyoxal and formaldehyde. *Food Hydrocolloids*, 2004; 18(5): 717e726.
7. Delgado-Vargas, F., & Paredes-Lopez, O. *Natural colorants for food and nutraceutical uses*. CRC press, 2002.
8. Gao, R., Hu, H., Shi, T., Bao, Y., Sun, Q., Wang, L., ... & Yuan, L. Incorporation of gelatin and Fe²⁺ increases the pH-sensitivity of zein-anthocyanin complex films used for milk spoilage detection. *Current Research in Food Science*, 2022; 5: 677-686.
9. Ghanbarzadeh, B., & Almasi, H. Physical properties of edible emulsified films based on carboxymethyl cellulose and oleic acid. *International Journal of Biological Macromolecules*, 2011; 48: 44–49.
10. Ghaani, M., Cozzolino, C. A., Castelli, G., & Farris, S. An overview of the intelligent packaging technologies in the food sector. *Trends in Food Science & Technology*, 2016; 51: 1–11.
11. Guo, J., Ge, L., Li, X., Mu, C., & Li, D. Periodate oxidation of xanthan gum and its crosslinking effects on gelatin-based edible films. *FoodHydrocolloids*, 2014; 39: 243–250.
12. Hazirah, M. N., Isa, M. I. N., & Sarbon, N. M. Effect of xanthan gum on the physical and mechanical properties of gelatin-carboxymethyl cellulose film blends. *Food Packaging and Shelf Life*, 2016; 9: 55-63.
13. Hu, H., Yao, X., Qin, Y., Yong, H., & Liu, J. Development of multifunctional food packaging by incorporating betalains from vegetable amaranth (*Amaranthus tricolor* L.) into quaternary ammonium chitosan/fish gelatin blend films. *International Journal of Biological Macromolecules*, 2020; 159: 675–684.
14. Kaur, K., & Kaushal, P. Enzymes as analytical tools for the assessment of food quality and food safety. In *Advances in Enzyme Technology*, 2019; 273-292. Elsevier.

15. Khan, P. M. A., & Farooqui, M. Analytical applications of plant extract as natural pH Indicator: a review. *Journal of advanced scientific research*, 2011; 2(04): 20-27.
16. Khazaei, A.; Nateghi, L.; Zand, N.; Oromiehie, A.; Garavand, F. Evaluation of Physical, Mechanical and Antibacterial Properties of Pinto Bean Starch-Polyvinyl Alcohol Biodegradable Films Reinforced with Cinnamon Essential Oil. *Polymers*, 2021; 13: 2778.
17. Koshy, R. R., Koshy, J. T., Mary, S. K., Sadanandan, S., Jisha, S., & Pothan, L. A. Preparation of pH sensitive film based on starch/carbon nano dots incorporating anthocyanin for monitoring spoilage of pork. *Food Control*, 2021; 126: 108039.
18. Kuswandi, B., Larasati, T. S., Abdullah, A., & Heng, L. Y. Real-time monitoring of shrimp spoilage using on-package sticker sensor based on natural dye of curcumin. *Food Analytical Methods*, 2012; 5: 881-889.
19. Kuswandi, B., Restyana, A., Abdullah, A., Heng, L. Y., & Ahmad, M. A novel colorimetric food package label for fish spoilage based on polyaniline film. *Food control*, 2012; 25(1): 184-189.
20. Kuswandi, B., Asih, N. P., Pratoko, D. K., Kristiningrum, N., & Moradi, M. Edible pH sensor based on immobilized red cabbage anthocyanins into bacterial cellulose membrane for intelligent food packaging. *Packaging Technology and Science*, 2020; 33(8): 321-332.
21. Mohebi, E.; Marquez, L. Intelligent packaging in meat industry: An overview of existing solutions. *J. Food Sci. Technol*, 2015; 52: 3947–3964.
22. Musso, Y. S., Salgado, P. R., & Mauri, A. N. Smart gelatin films prepared using red cabbage (*Brassica oleracea* L.) extracts as solvent. *Food Hydrocolloids*, 2019; 89: 674-681.
23. Prietto, L., Mirapalhete, T. C., Pinto, V. Z., Hoffmann, J. F., Vanier, N. L., Lim, L. T., ... & da Rosa Zavareze, E. pH-sensitive films containing anthocyanins extracted from black bean seed coat and red cabbage. *Lwt*, 2017; 80: 492-500.
24. Realini, C.E.; Marcos, B. Active and intelligent packaging systems for a modern society. *Meat Sci*, 2014; 98: 404–419.
25. Rhim, J.-W., Park, H.-M., & Ha, C.-S. Bio-nanocomposites for food packaging applications. *Progress in Polymer Science*, 2013; 38: 1629–1652.
26. ruRong, L., Zhang, T., Ma, Y., Wang, T., Liu, Y., & Wu, Z. An intelligent label using sodium carboxymethyl cellulose and carrageenan for monitoring the freshness of fresh-cut papaya. *Food Control*, 2023; 145: 109420.

27. Rotariu, L., Lagarde, F., Jaffrezic-Renault, N., & Bala, C. Electrochemical biosensors for fast detection of food contaminants – Trends and perspective. *Trac-Trends in Analytical Chemistry*, 2016; 79: 80–87.
28. Saha, Supradip, Jashbir Singh, Anindita Paul, Rohan Sarkar, Zareen Khan, and Kaushik Banerjee. "Anthocyanin profiling using UV-vis spectroscopy and liquid chromatography mass spectrometry." *Journal of AOAC International*, 2020; 103, 1: 23-39.
29. Sani, M.A.; Azizi-Lalabadi, M.; Tavassoli, M.; Mohammadi, K.; McClements, D.J. Recent Advances in the Development of Smart and Active Biodegradable Packaging Materials. *Nanomaterials*, 2021; 11: 1331.
30. Sani, M.A.; Tavassoli, M.; McClements, D.J.; Hamishehkar, H. Multifunctional halochromic packaging materials: Saffron petal anthocyanin loaded-chitosan nanofiber/methyl cellulose matrices. *Food Hydrocoll*, 2021; 111: 106237.
31. Shao, P., Liu, L., Yu, J., Lin, Y., Gao, H., Chen, H., & Sun, P. An overview of intelligent freshness indicator packaging for food quality and safety monitoring. *Trends in Food Science & Technology*, 2021; 118: 285–296.
32. Slavin, J.L.; Loyd, B. Health Benefits of Fruits and Vegetables. *Adv. Nutr*, 2012; 3: 506–516.
33. Sohail, M., Sun, D.-W., & Zhu, Z. Recent developments in intelligent packaging for enhancing food quality and safety. *Critical Reviews in Food Science and Nutrition*, 2018; 58(15): 2650–2662.
34. Tavassoli, M.; Sani, M.A.; Khezerlou, A.; Ehsani, A. McClements DJ. Multifunctional nanocomposite active packaging materials: Immobilization of quercetin, lactoferrin, and chitosan nanofiber particles in gelatin films. *Food Hydrocoll*, 2021; 118: 106747.
35. Warsiki, E., & Rofifah, N. Dragon fruit freshness detector based on methyl red colour indicator. *IOP Conference Series: Earth and Environmental Science*, 2018; 209: 012016.
36. Zam, M., Niyumsut, I., Osako, K., & Rawdkuen, S. Fabrication and Characterization of Intelligent Multi-Layered Biopolymer Film Incorporated with pH-Sensitive Red Cabbage Extract to Indicate Fish Freshness. *Polymers*, 2022; 14(22): 4914.